REPORT DOCUMENTATION PAGE

AFRL-SR-BL-TR-98-

0735

1. AGENCY USE ONLY (Leave Blank)	2. REPORT DATE	3. REPORT TYPE AND DATES COVERED
	December 5, 1990	Final

4. TITLE AND SUBTITLE
A Study of the Interfacial Properties of an $Al/Al_3Zr_xTi_{1-x}$ Metal Matrix Composite

5. FUNDING NUMBERS

6. AUTHORS
Philip A. Earvolino

7. PERFORMING ORGANIZATION NAME(S) AND ADDRESS(ES)
Northwestern University

8. PERFORMING ORGANIZATION REPORT NUMBER

9. SPONSORING/MONITORING AGENCY NAME(S) AND ADDRESS(ES)
AFOSR/NI
4040 Fairfax Dr, Suite 500
Arlington, VA 22203-1613

10. SPONSORING/MONITORING AGENCY REPORT NUMBER

11. SUPPLEMENTARY NOTES

12a. DISTRIBUTION AVAILABILITY STATEMENT
Approved for Public Release

12b. DISTRIBUTION CODE

13. ABSTRACT *(Maximum 200 words)*
See Attachment

14. SUBJECT TERMS

15. NUMBER OF PAGES

16. PRICE CODE

17. SECURITY CLASSIFICATION OF REPORT	18. SECURITY CLASSIFICATION OF THIS PAGE	19. SECURITY CLASSIFICATION OF ABSTRACT	20. LIMITATION OF ABSTRACT
Unclassified	Unclassified	Unclassified	UL

NORTHWESTERN UNIVERSITY

A Study of the Interfacial Properties of an $Al/Al_3Zr_xTi_{1-x}$ Metal Matrix Composite

A RESEARCH PROPOSAL

SUBMITTED TO THE GRADUATE SCHOOL

IN PARTIAL FULFILLMENT OF THE REQUIREMENTS

for the degree of

DOCTOR OF PHILOSOPHY

Field of Materials Science and Engineering

by

PHILIP A. EARVOLINO

Evanston, IL

December 5, 1990

Abstract

The $Al/Al_3Zr_xTi_{1-x}$ metal-matrix composite is unique. Unlike most MMC's, which are formed by chemical reaction of the reinforcing phase with the matrix, the intermetallic particles in this material develop by solidification. The particles are formed when a molten mixture of the elemental constituents in the composite is cast. The apparent result of this process is a particle/matrix interface of impressive strength. The composite has shown excellent ductility, but there has been no evidence of particle pullout or debonding. It is proposed that the mechanical properties and microscopic features of this composite be determined and compared to those found in materials with apparently brittle interfaces, e.g. Al/SiC. The properties will also be compared to those found in a composite of the same composition but prepared differently, i.e. by long-term, high temperature aging of supersaturated Al solid solutions containing small quantities of Zr and Ti. These comparisons will help to explain the interfacial strength of the $Al/Al_3Zr_xTi_{1-x}$ metal-matrix composite.

TABLE OF CONTENTS

1. Introduction

Metal-matrix composites (MMC's) are engineering materials which have begun to receive great attention. Though the mechanical properties of MMC's have, in many cases, been extensively studied, fundamental knowledge of the interfacial region in these composites is lacking. Determination of the extent to which this aspect of the composites affects their performance is the broad goal of this research. Mechanical strength, for example is largely determined by the bonding between a two-component material. The chemical stability of the interfacial region is of importance in its long-time performance. The defect structure of the region, e.g. particle-dislocation interactions, may determine the material's properties. Thus, rational design of a composite material requires an understanding of intrinsic interfacial behavior.

The material system consisting of $Al_3Zr_xTi_{1-x}$ crystallites in an Al matrix is a different type of composite. Unlike other metal matrix composites, which usually consist of metal alloys reinforced with ceramics, the $Al/Al_3Zr_xTi_{1-x}$ system is more accurately described as a "natural" composite. The intermetallics exist as equilibrium phases; the material is prepared by casting of a molten mixture of Al, Zr and Ti. Thus, the composite's interfacial properties are unique: the second phase develops upon solidification rather than by chemical reaction with the matrix material. In an as-cast condition, the particles are far too large (hundreds of microns) to confer strengthening by the means found in precipitation-hardened alloys, e.g. Orowan strengthening. Rather, strengthening in composites occurs by the transfer of load from the matrix to the reinforcing phase, which consists of large particles, fibers, whiskers, etc. Despite the size, as well as the brittleness, of the particles in the the $Al/Al_3Zr_xTi_{1-x}$ composite material, it has shown impressive ductility. Although particles are dramatically reduced in size during physical deformation of the sample, the particle/matrix interface apparently has considerable strength and it appears to "heal": there is no evidence of particle debonding or fallout.

Solidification of $Al_3Zr_xTi_{1-x}$ from the liquid phase is not the only way to manufacture this MMC. It has been shown that, from the melt, accelerated cooling rates result in a supersaturated solid solution of Zr and Ti in Al. Proper thermal and mechanical treatments of this solid produce (either directly or indirectly, *via* a metastable phase) the equilibrium intermetallic phase. It seems possible that long-term aging at high temperatures will result in particles of the same approximate size as those found in the heavily deformed composites above. The $Al/Al_3Zr_xTi_{1-x}$ composite therefore invites some interesting comparisons, not only between it and synthetic MMC's, but between the two methods of preparing the same material. The purpose of this research is to explore, by mechanical testing and microscopic analysis, the role the interface plays in distinguishing amongst the properties of these different species of composites.

2. Theoretical Background

2.1 Present MMC's

Synthetic MMC's are most frequently prepared by chemical reaction of the reinforcing phase with the matrix material. The result is often a reaction zone, which may adversely affect the composite's properties. A common example is the Al/SiC MMC. Possible reaction products are Al_4C_3, and Al_2O_3 (from reduction of the silicon oxide layer at the surface of the SiC), and MgO if Mg is present in the Al alloy[1, 2]. The resulting reaction zone is brittle and acts as a preferred site for crack initiation. Additionally, the formation of reaction products has been used as an explanation for the poor abrasive wear of Al/SiC composites due to the weakness of the brittle interface[3]. The presence of a reaction zone is not expected in the $Al/Al_3Zr_xTi_{1-x}$ system, in which equilibrium solidification produces the second phase, or in which coarsening creates large particles.

Another example of the poor bonding at a metal-ceramic interface is the Al/Al_2O_3 system. Elastic moduli of composites with various fractions of second phase show only small increases over the modulus of the Al matrix, in spite of the much larger modulus of alumina[4].

Furthermore, Clegg, et. al[5] have shown that composites of 99.99% Al reinforced with Al_2O_3 fibers demonstrate brittle fracture behavior. The bonding in this system is largely ionic in character, whereas metallic bonding predominates in metal matrices reinforced with intermetallics. It has been suggested[6] that there may be less tendency for fatigue crack initiation at the interface if it is characterized by metallic bonding rather than by covalent or ionic bonding. For example, fatigue cracks initiate at the Al/Al_2O_3 interface[7, 8], but not at the Fe/Fe_3C interface[9]. For these reasons, the $Al/Al_3Zr_xTi_{1-x}$ system may offer promise in areas where other MMC's have failed. Indeed, the ductility already shown by the composite encourages optimism.

2.2 Materials Selection

The materials chosen for this study were originally selected in a search for high-temperature aluminum alloys. In this application, fine thermodynamically stable particles which resist coarsening at elevated temperatures are desired. By minimizing the lattice disregistry across the particle/matrix interface, the interfacial energy would, presumably, be lowered. This, in turn, would reduce the driving force for particle growth by Ostwald ripening. Fine[10] suggested a variety of intermetallic compounds which might satisfy these conditions. Two of these, Al_3Zr and Al_3Ti, possess tetragonal crystal structures with lattice mismatches along the a-axis of approximately 1% and 5%, respectively, compared to the lattice parameter of FCC aluminum[11]. Furthermore, owing to the solid solubility between these two compounds, it seemed probable that a mixed crystal of the type $Al_3Zr_xTi_{1-x}$ could be formed.

Phase diagrams of the Al-Zr and Al-Ti systems are given in Figures 1 and 2[12]. At the aluminum-rich end of both diagrams, the $Al_3(Zr, Ti)$ compound reacts peritectically with liquid Al to form a solid solution:

$$Al(l) + Al_3(Zr, Ti) \rightarrow Al(ss)$$

The maximum solid solubility of Zr in Al is strongly temperature-dependent. At 663°C, the solubility is 0.083 a/o (0.28 w/o) Zr. At 20°C, the value is 0.012 a/o (0.03 w/o). The maximum solubility for Ti in Al is 0.57 - 0.68 a/o (1.0 - 1.2 w/o) at the peritectic temperature (660.5°C) and it decreases with temperature as well.[13]

The Al_3Ti intermetallic compound is of the DO_{22} crystal structure. The unit cell contains 6 Al atoms and 2 Ti atoms. The Al_3Zr compound possesses the DO_{23} crystal structure, the unit cell of which has 12 Al atoms and 4 Zr atoms. Essentially, the DO_{23} crystal is formed by taking a DO_{22} unit cell and placing an inverted DO_{22} unit cell on top of it. Both the DO_{22} and DO_{23} structures are shown in Figure 3, along with the FCC unit cell of aluminum. As may be observed, both the DO_{22} and DO_{23} structures are FCC-derivative[14].

Tsunekawa and Fine[15] explored the crystal structure of the mixed crystal intermetallic compound $Al_3Zr_xTi_{1-x}$. Lattice parameters for both the intermetallic compound and the aluminum solid solution in Al-2 at.% (Ti + Zr) alloys were determined by x-ray crystallography. The values determined are plotted as a function of x in Figure 4. The parameter c in the tetragonal phase is compared to $4a_o$, where a_o is the lattice parameter of the Al solid solution formed by minimal solubility of Zr and Ti atoms; a_o differs from the parameter of pure Al by only about 0.1%. They determined that the crystal structure is DO_{23} for values of x greater than or equal to 0.25 and DO_{22} for $x < 0.11$. For the range $0.11 < x < 0.25$, apparently both structures may form. As may be seen in Figure 5[11], the overall mismatch was approximately the same for all values of $x > 0.25$. The overall mismatch is simply an average of mismatches for all parameters; it is defined as:

$$\delta = [100/3]\left\{2\left|\left(1 - \frac{a(Al_3X)}{a_0(Al)}\right)\right| + \left|\left(1 - \frac{c(Al_3X)}{na_0(Al)}\right)\right|\right\}$$

where n = 4 for DO_{23}-type structures.

Although the present concern is not high-temperature alloys, the properties of the particle/matrix interface are of clear importance in the development of metal matrix composites: most composites appear to fail in this region. Thus, even for particles of the tetragonal phase, coherent or semi-coherent interfaces may offer strength and effective load transfer from particle to matrix.

Another property of concern for second phase particles in metal matrix composites is their ductility. Sawamura [16] has shown that, in the $Al_3Zr_xTi_{1-x}$ intermetallic of DO_{23} structure, resistance to cracking is improved by minimizing x. Increased ductility in the intermetallic particles should improve the composite's tensile and creep properties.

3. Work To-Date

3.1 Sample Preparation

Samples of the $Al/Al_3Zr_xTi_{1-x}$ metal matrix composite have been prepared by nonconsumable tungsten arc-melting under an argon atmosphere, with a water-cooled copper crucible used as the cathode. Initial components are chips of 99.999% Al, granules of 99.9% Ti, and shavings of 99.9% Zr. The melted buttons are flipped ten times to insure compositional homogeneity. The drawbacks of this method are twofold: porosity in the as-cast materials is high, in some cases as much as 25%; and, the largest sample which can be produced with the available apparatus weighs 12g. The intermetallic particles in the as-cast structure are plate-like; in a composite with 15 volume percent particles, the largest ones may be over 200 μm long but only 6 μm thick (see Figure 6). They are tetragonal, of the DO_{23} structure, as confirmed by x-ray diffractometry.

The arc-melted composite has shown considerable ductility, in spite of the porosity. An $Al\text{-}Al_3Zr_{0.25}Ti_{0.75}$ (15v/o) has been hot-pressed (500 °C) to a final reduction of 59% and then successively cold-rolled to a final reduction of 95% (a thickness of 0.50 mm). Longitudinal and long transverse sections of this sample are shown in Figures 7 and 8. The particles have been reduced considerably in size: in the rolling plane, the platelets have widths

of no greater than 15 μm. The transverse section shows that the particles have thicknesses no greater than 6 μm. Further rolling of this sample resulted in a total reduction of 99.74% (a thickness of 26μm). By folding this foil and rolling it, an effective reduction of 99.983% has been achieved. After this extreme deformation, though, particles appear to be no smaller than they were at 95% reduction.

3.2 Transmission Electron Microscopy

An arc-melted Al-$Al_3Zr_{0.75}Ti_{0.25}$ (15v/o) sample was prepared for microscopy as follows. The sample was hot-pressed (500°C) to a reduction of 60% and then cold-rolled to a thickness of 120 μm, representing a total reduction of 98.8%. From the resulting sheet of material, 3mm discs were cut on an electric discharge machine. These discs were then polished on 600 grit paper to a final thickness of 60 μm. Finally, these were jet polished using an etchant of 2.7% perchloric acid (70%), 36% n-butyl alcohol, and 61% methyl alcohol, by volume at a temperature of -27°C. A Fischione polisher was used; the polishing conditions were 14 V and 8 mA. As this solution is specific for the intermetallic, the Al matrix was still thick and was thinned further by argon ion-milling at an incidence angle of 10° for one hour.

Figure 9 is a TEM micrograph of the sample prepared above. The particle/matrix interface appears to be sharp and continuous. The diffraction pattern of the particle is also included (Fig. 10). By indexing this pattern, the lattice parameters of the intermetallic particle may be determined if the camera constant is known. This value, determined previously, is 13.86 mmÅ. The lattice parameter values were then calculated as c = 16.53Å and a = 4.110 Å. Compared to the results of Tsunekawa and Fine[15], these represent errors of 2.01% and 1.49%, respectively. Due to the error in the camera constant, which was obtained previously and may differ from the true value at the time the photograph was taken, the error in these values seems reasonable.

3.3 Matrix Strength

The matrix strength in the $Al/Al_3Zr_xTi_{1-x}$ system was determined using a method first described by Argon, et al.[17, 18, 19] to determine interfacial bond strengths in spheroidized 1045 steel, Cu-0.6% Cr alloy and and maraging steel containing various carbides. Flom and Arsenault later used this approach to determine interfacial strength in an Al-SiC composite[20]. In all of these materials, fracture occurs by nucleation and growth of voids at the particle/matrix interface due to decohesion. Nucleation of the voids is promoted by the imposition of a state of triaxial tensile stress. From the theoretical bonding analysis of Argon et al.[18], the interfacial stress σ_{rr} can be expressed as:

$$\sigma_{rr} = \sigma_T + Y(\bar{e}^p)$$

where σ_T is the local triaxial tensile stress and $Y(\bar{e}^p)$ is the true flow stress in tension corresponding to the local average plastic strain, had the particle been absent. The assumptions of this analysis are: the particles are of equiaxed shape; the volume fraction of particles is small; and, the particles are undeformed. The triaxial tensile stress distribution along the radius in the plane of the tensile specimen notch may be expressed as:

$$\frac{\sigma_T}{\sigma_0} = \frac{c}{\left\{1 - \left(r/a'\right)^2\right\}^{1/2}}$$

where σ_T/σ_0 is the triaxiality, σ_T is the negative pressure, σ_0 is the flow stress (average ligament stress), z is the vertical distance along the tensile axis of the specimen, and r is the distance from the z axis. Triaxiality is maximized when $r = a$ (i.e. at the notch); $2a$ is the ligament diameter. Parameters c and a' are defined as:

$$c = \frac{1 + a/R + \left(1 + a/R\right)^{1/2}}{2\left\{2 + a/R + \left(1 + a/R\right)^{1/2}\right\}}$$

$$a' = \frac{a(1 + a/R)}{a/R}$$

where a is the radius of the ligament and R is the radius of the groove (see Figure 11).

For the present study, two 12g samples were prepared by arc-melting: Al-$Al_3Zr_{0.25}Ti_{0.75}$ (3v/o) and Al-$Al_3Zr_{0.5}Ti_{0.5}$ (3v/o). They were swaged to a final diameter of 0.312 in (a reduction in cross-sectional area of 80%). Each of these rods was then electric discharge machined to produce specimens for tensile testing (Fig. 12). Specimens were tested in tension to fracture on an Instron model 1125 machine. The cross-head speed was 10^{-3} in s^{-1}.

By determining the stress at fracture, a lower bound value for the interfacial strength may be obtained; the actual value is either higher or equal to this. This, of course, assumes void nucleation at the particle/matrix interface. For the samples tested above, however, fracture of the composite occurred in the matrix. Thus, a value for *matrix* strength is obtained. The average value for the Al-$Al_3Zr_{0.25}Ti_{0.75}$ (3v/o) system was 411 MPa; for the Al-$Al_3Zr_{0.5}Ti_{0.5}$ (3v/o) system, the value was 442 MPa. SEM micrographs of the fracture surface are indicative of ductile fracture (Figure 13). They do *not* show fracture at the particle-matrix interface; hence, a value for the strength of the interface can not be determined explicitly.

3.4 Elastic Modulus

The elastic moduli of composites of varying compositions were determined by a dynamic method. The modulus of a material is related to the resonant frequency of a displacement wave travelling through it by the relation:

$$E = \frac{4L^2 \rho f_n^2}{n^2}$$

where L is the length of the sample, r is its density, f_n is its resonant frequency, and n is the number of zero-displacement nodes in the sample (for this experiment, assumed to equal one). If the material is cut in the form of a rectangular slab and clamped at one end to a piezoelectric crystal of known resonant frequency, then the resonant frequency of the slab of material will be given by:

$$f_S = f_C + (M_X/M_S)(f_C - f_X)$$

where f_S is the resonant frequency of the material sample, f_C is the resonant frequency of the composite system, M_X is the the mass of crystal, M_S is the mass of the sample, and f_X is the resonant frequency of the crystal[21].

The modulus values obtained from this method are plotted against the fraction of intermetallic in the composite (Fig. 14 and Fig. 15). Moduli values predicted by two theoretical models deserve comparison[4]. Voight averaging assumes uniform strain in both phases, resulting in a modulus which is a weighted average of the moduli of the components:

$$E_{Voigt} = X_{Al_3Zr_xTi_{1-x}} E_{Al_3Zr_xTi_{1-x}} + X_{Al} E_{Al}$$

where x is the volume fraction of the component and E is its Young's modulus. This is simply the linear rule of mixtures. Reuss averaging assumes uniform stress in both phases, leading to a modulus given by:

$$E_{Reuss} = \frac{1}{\frac{X_{Al_3Zr_xTi_{1-x}}}{E_{Al_3Zr_xTi_{1-x}}} + \frac{X_{Al}}{E_{Al}}}$$

Presumably, weak or discontinuous interfaces will lead to lowering of experimental moduli values; hence, poorer transfer of either stress or strain, and greater deviation from the

ideal case predicted by either model. The moduli values obtained by Voight averaging are shown in Figs. 14 and 15. Zedalis, et al.[22] showed that moduli values for the Al/Al_3Zr system prepared by arc-melting followed the linear relationship predicted by Voight averaging. Moduli of samples containing 5, 10, 15 and 25 v/o Al_3Zr were determined by sound velocities. The plot of E vs. fraction of Al_3Zr showed a linear coefficient of correlation of 0.96. Thus it is expected that the $Al/Al_3Zr_xTi_{1-x}$ system will obey a linear law.

Plots are given for two different composite systems: $Al/Al_3Zr_{0.5}Ti_{0.5}$ and $Al/Al_3Zr_{0.25}Ti_{0.75}$. All of the samples tested were hot-pressed and cold-rolled to a total reduction of approximately 80%. Although this breaks up particles and partially destroys the native interface, the cold-working was necessary to reduce porosities to values where their effect upon modulus was negligible. Indeed, modulus values for as-cast samples were shown to decrease in a roughly linear (correlation coefficient of 0.92) fashion with porosity fraction (Fig. 16). Deviation from the Voight average may be explained by the partial destruction of the interface. More measurements, perhaps on samples possessing higher percentages of intermetallic, are needed to determine the extent of debonding as a function of cold work.

3.5 Creep Testing

$Al/Al_3Zr_{0.75}Ti_{0.25}$.(15 v/o) samples were rolled to a final thickness of approximately 0.5 mm (95% reduction) and annealed 3 hrs. at 425°C. They were then dead-load crept at 10 MPa (initial) stress. The average steady creep rate obtained for two samples was 1.6×10^{-5}. This is not an impressive value, *per se*, but the steady creep rate of pure (99.99%) Al at 10 MPa is only about 10^{-1}[23]. Apparently, the creep properties of pure Al are *so* poor that even if a great fraction of the load is transferred from the matrix to the intermetallic, the overall creep strength of the composite is still reduced by the matrix. Future creep testing must involve a strengthened matrix, e.g. a solution-hardened Al alloy.

4. Proposed Research

4.1 Sample Preparation

All samples which have been prepared to-date have contained large fractions of intermetallic particles. In the as-cast condition, these particles may be over 200 μm long. Any reduction in particle size has been obtained by severe physical deformation of the sample. Therefore, the native particle/matrix interface no longer exists. Microscopy of the deformed samples, however, has shown that the interface apparently heals. This likely explains the impressive ductility shown by the composite. Quantitative analysis of the interface has not yet been possible. What is now desired is an $Al/Al_3Zr_xTi_{1-x}$ composite possessing a *native* interface. The properties of such a material may then be directly compared to those in the deformed sample.

Zedalis [11] has shown that the stable tetragonal DO_{23} phase may be directly precipitated from a supersaturated solid solution of Al-0.75 w/o Zr prepared by arc-melting. If the as-cast button is 90% cold-rolled, preaged at 600°C for 50 hours, and isothermally aged at 425°C, the stable phase apparently precipitates *directly* from solution without first forming metastable $L1_2$ particles. This was an interesting result because early reports[24, 25] had shown the presence of a fairly stable $L1_2$ phase. Ryum showed that the equilibrium DO_{23} structure occurs via the intermediate $L1_2$ phase; aging at 500°C for 120 hours resulted in the equilibrium crystallography. These particles formed mostly at grain boundaries and occasionally in the matrix as well[26]. Zedalis found that the coarsening rate showed either a r^2 or r^3 dependence, where r is the average particle radius.

From Zedalis' work, it appears that a sample containing only the stable tetragonal DO_{23} phase may be prepared. Some important modifications will be made, however, for the present system. At 425°C, particles were only 500 nm long (60 nm radius) even after 400 hours aging. To obtain particles on the order of 5 to 10 μm long, this temperature will have to be raised, perhaps to 500°C or greater. Finally, the systems studied by Zedalis produced only one volume percent particles. It is likely that if this value is to be raised to 5 or 10 percent, the cooling rate in the sample solidification process will need to be increased. This will be made

possible by the design of a new copper crucible geometry. Presently, samples cool in long cylindrical horizontal slots. A configuration which increases the surface area-to-volume ratio will provide enhanced cooling rates. Although it may not be possible to produce a supersaturated solid solution without precipitates, it should minimize the number of $L1_2$ particles and reduce the size of stable tetragonal particles in the as-cast sample. At any rate, if a supersaturated solid solution is formed, some coarsening will be possible. Haugan, et al. [27] have shown that for Al-Al_3Zr (2 v/0) arc-melted in a wedge-shaped copper crucible, cooling rates of 100°C s^{-1} or less produce stable Al_3Zr particles without also causing the metastable form to precipitate. Cooling rates which are too low, however, will not sufficiently supersaturate the Al solid solution.

Manufacture of samples containing large tetragonal particles has been achieved with samples containing 15 or 25 v/o second phase. As described above, these samples have shown considerable ductility, and extensive cold rolling has produced samples with particles on the order of 10 μm or less. This has required 99.99% reduction in thickness. Samples containing only 10 or less percent precipitate should possess smaller particles in the as-cast condition than those found in the 15 v/o composites previously produced. Thus, less reduction in thickness will be required.

By careful sample preparation and the appropriate deformation, samples possessing particles of roughly equal size will be obtained. Proper heat treatments will then be necessary to obtain equivalent grain sizes in both types of sample. The end result of these procedures will be two types of material, as similar as possible in all respects except for the condition of the particle/matrix interface: in one class of material, the interface will be in its "native", post-coarsening state; in the other, the interface will have formed after severe deformation of the sample.

4.2 Mechanical Testing

4.2.1 Tension Testing

Tension testing of each class of material will provide values for the ultimate tensile strength, the yield strength and the percent elongation. In both varieties of composite, these characteristics will be obtained for various Zr/Ti ratios. For the deformed samples (henceforth designated as Type "A"), the effect of particle size and volume fraction of second phase particles will be determined. SEM analysis of the fracture surfaces will reveal the location of cracks and the direction of their growth, as well as the presence of particle/matrix debonding. Due to the low strength of pure aluminum (yield strength of 10 MPa, 50% elongation in tension for 99.99% Al), the composite matrices may be alloyed with 5 w/o Mg to produce improved properties via solid solution strengthening. Al-5 w/o Mg has a yield strength of 155 MPa and 25% elongation in tension[28]. This should reduce considerably the likelihood of matrix cracking, which was previously observed in interfacial strength testing.

Comparison of the results of this testing with those found for Al/SiC composites should be revealing. In the latter system, a debate regarding the nature of the relevant strengthening mechanism exists. Nardone and Prewo have applied a modified shear lag theory to the problem of short fiber composites and subsequently explained the strengthening of Al/SiC_w composites by shear lag strengthening (i.e. by a continuum mechanics treatment of load transfer)[29]. On the other hand, Arsenault has attributed the strength of the composite to, primarily, high dislocation density arising from cooling of the system following heat treatment[30]. As will be explained below, this dislocation density may not exist in the $Al/Al_3Zr_xTi_{1-x}$ system; therefore, load transfer may be the primary, if not exclusive, mode of strengthening in this MMC.

4.2.2 Creep Testing

The creep behavior of metal matrix composites, particularly aluminum alloys reinforced with SiC whiskers, has been an area of considerable interest recently. As opposed to oxide dispersion strengthened (ODS) alloys, the particles in the MMC's are generally too large ($\approx$ 5 μm) and the interparticle spacing is too great to enable Orowan strengthening[31, 32]. As a

result, the load transfer from matrix to the stiffer particles has been proposed as a significant strengthening mechanism. Morimoto, et al.[33] have indicated the effect of debonding or partial debonding on creep resistance. Goto and McClean[34] have proposed a model which accounts for the degree of bonding at the interface. Their calculations predict that a weak, slipping interface may reduce creep rates by several orders of magnitude. Additionally, Al alloys reinforced with SiC whiskers show better (by one or two orders of magnitude) steady state creep rates than those reinforced with particulate SiC, owing to the whiskers' greater effectiveness in bearing loads[32, 35]. Two other strengthening mechanisms have been described for SiC whiskers which may not be relevant for the $Al/Al_3Zr_xTi_{1-x}$ system: 1) the Al/SiC_w composite shows a large capacity for work hardening, an effect which diminishes with temperature; and, 2) an attractive particle/dislocation interaction due to the incoherent interface may enhance creep strength[31].

A comparison of creep properties of the two classes of materials may indicate the effectiveness of the interface in transmitting load to the interface. A direct comparison of the performance of class A materials with the "native" interface composites (class B) will provide information on the integrity of the interface after physical deformation. Again, SEM analysis of the fracture surfaces, as well as optical microscopy, will reveal the degree of particle debonding. The enhancement of matrix strength by alloying with magnesium may again be necessary, as the creep properties of pure aluminum are poor. TEM of crept specimens will provide useful information on particle/dislocation interactions, and the degree of coherency. Unlike the Al alloy/SiC system, no reaction zone between particle and matrix is expected.

4.2.3 Interfacial Strength

The test developed by Argon will be used to determine, once again, the interfacial strength in the $Al/Al_3Zr_xTi_{1-x}$ composite. This time, the matrix will be strengthened by addition of 5 w/o Mg. The Al-Mg alloy will be used as a starting component; it will be

obtained elsewhere. This will hopefully reduce the likelihood of matrix failure, which invalidated the previous test.

4.2.4 Nanoindentation

The nanoindenter at Sandia National Laboratories will be used to obtain values of particle and matrix hardness. Stress-strain relationships in the vicinity of particles will show if, and to what extent, work hardening due to high dislocation density exists. These data will be compared to those in Al/SiC, where high dislocation densities are known to exist[30].

4.2.5 Elastic Modulus

As mentioned previously, it has been proposed that moduli values are higher in those composites with strong interfaces (which will effectively transfer stresses and strains from the matrix to the second phase particles). Thus, a direct comparison of the interfacial strengths in types A and B composites is possible. The modulus of aluminum is *not* affected by the degree of cold work [28]. Thus, controlling grain size will not be as important in determining moduli values as it is in the other mechanical tests mentioned previously. Porosity, however, does have a strong effect on the modulus. Fortunately, both classes of material will have been rolled (in one case to promote precipitation, in the other to reduce particle size). This has been shown to reduce the sample porosity to under 2%.

4.2.6 Transmission Electron Microscopy

TEM will be used to explore the structure of the particle/matrix interface in both the coarsened and fractured particles. In particular, the nature of particle-dislocation interactions will be studied primarily by weak beam techniques. Dislocation structure may have a profound effect on the composite strength. In Al-alloys reinforced with SiC whiskers, part of the ultimate strength has been attributed to the high dislocation density at the particle/matrix interface. The dislocations arise upon cooling of the sample from some processing

temperature; the coefficients of thermal expansion between the aluminum and the SiC are drastically different (about a factor of 10)[30]. Such high dislocation densities are not expected in the $Al/Al_3Zr_xTi_{1-x}$ system: the difference in coefficients of thermal expansion is probably less and the interface is expected to be semicoherent, as opposed to the incoherent Al/SiC interface, a low energy site for dislocations. The presence of an orientation relationship between particle and matrix will be explored. Izumi and Oelschlägel[24] showed a relationship of the form:

$$<001>_{Al_3Zr} // <001>_{Al} \qquad (100)_{Al_3Zr} // (100)_{Al}$$

for the equilibrium tetragonal phase Al_3Zr particles in an Al matrix.

If time permits, EELS techniques will be used to investigate possible chemadsorption at the interface. High resolution electron microscopy (HREM) will be used to produce atomic images of the interface and particles. Lattice images of Al_3Zr (DO_{23}) particles have been obtained at Northwestern University before, but on particles roughly two orders of magnitude smaller than those found in the samples to be tested in this research[36].

Preparation of this composite material for electron microscopy has proven to be difficult. Improved techniques, particularly in mechanical polishing, must be used. Electropolishing has been used with some success to thin the sample. Newer techniques, however, involving acidless electropolishing may offer promise, particularly for the thinning of the intermetallic particles[37]. Ion milling will be used to eliminate surface contamination.

5. Conclusion

The particle/matrix interface in the $Al/Al_3Zr_xTi_{1-x}$ composite is unique. It is important in the material's manufacture (i.e. either when particles coarsen or when they solidify) and in its mechanical behavior, where the effectiveness of load transfer is of extreme importance. It is proposed that the interface in this system may be explored in two conditions. In the first, the intermetallic phase has coarsened due to isothermal aging at high temperature. In such a state,

the interface may be said to exist in a "native" state. In the second condition, the particles have been formed by solidification and then have been greatly reduced in size due to extreme deformation of the material. Here, the interface is mostly, if not exclusively, new. Direct comparison , by microscopic investigation and mechanical testing, of the two classes of material thus formed will provide information on the strength and integrity of the interface which exists after deformation. In addition, comparison to other MMC's will help explain the *unique* role of the interface in the $Al/Al_3Zr_xTi_{1-x}$ composite.

REFERENCES

1. G. Elkabir, "High Energy-High Rate Powder Processing of Aluminum Silicon Carbide Metal Matrix Composites," PhD Thesis, University of Texas (1987).

2. H. Marcus and L. K. Rabenberg, "Interface Characteristics and Mechanical Properties of Metal-Matrix Composites," *(Technical Report UTCMSE-87-3)* ONR, (1987).

3. K. J. Bhansali and R. Mehrabian, "Abrasive Wear of Aluminum-Matrix Composites," *J. Metals* **34** (1982) 30-32.

4. M. E. Fine, "Elastic Moduli of Two Phase Aluminum Alloys," *Scripta Met.* **15** (1981) 523-524.

5. W. J. Clegg, et al., "The Tensile Deformation and Fracture of Al-"Saffil" Metal-Matrix Composites," *Acta Met.* **36** (1988) 2151-2159.

6. M. E. Fine and J. R. Weertman, "Tailored Interfaces for Metal-Matrix Composites--Fundamental Considerations," *(grant to support basic research (AFOSR))* Department of Materials Science and Engineering, Northwestern University, (1988).

7. D. R. Williams, "Fatigue Crack Initiation and Microcrack Growth in Silicon Carbide Whisker Reinforced 2124 Aluminum Alloy," PhD Thesis, Northwestern University (1985).

8. N. M. A. Eid and R. F. Thomason, "The Nucleation of Fatigue Cracks in a Low-alloy Steel Under High-Cycle Fatigue Conditions and Uniaxial Loading," *Acta Met* **27** (1979) 1239.

9. H. Sunwoo, et al., "Cyclic Deformation of Pearlitic Eutectoid Rail Steel," *Met. Trans.* **13A** (1982) 2035.

10. M. E. Fine, "Precipitation Hardening of Aluminum Alloys," *Met. Trans.* **6A** (1975) 625-630.

11. M. S. Zedalis, "Development of an Elevated Temperature Aluminum Alloy Containing Al_3X-Type Dispersed Phases," PhD Thesis, Northwestern University (1985).

12. T. B. Massalski, "Binary Alloy Phase Diagrams," in: ed., ASM, Metals Park, OH (1986) .

13. V. M. Glazov, G. Lazarev and G. Korolkov, "The Solubility of Certain Transition Metals in Aluminum," *Metalloved. i Term. Obrabotka Metal.* **10** (1959) 48-50.

14. A. E. Carlsson and P. J. Meschter, "Relative Stability of $L1_2$, DO_{22}, and DO_{23} structures in MAl_3 Compounds," *J. Mater. Res.* **4** (1989) 1060-1063.

15. S. Tsunkewa and M. E. Fine, "Lattice Parameters of Al_3 (Zr_xTi_{1-x}) vs. x in Al-2 at.% (Ti + Zr) Alloys," *Scripta Met.* **16** (1982) 391-392.

16. I. Sawamura, "High Temperature Deformation Properties of Al_3Ti-base Intermetallic Compounds," *(proposal for PhD research)* Northwestern University, (1990).

17. A. S. Argon, J. Im and A. Needleman, "Distribution of Plastic Strain and Negative Pressure in Necked Steel and Copper Bars," *Met. Trans.* **6A** (1975) 815-824.

18. A. S. Argon, J. Im and R. Safoglu, "Cavity Formation from Inclusions in Ductile Fracture," *Met. Trans.* **6A** (1975) 825-838.

19. A. S. Argon and J. Im, "Separation of Second Phase Particles in Spheroidized 1045 Steel, Cu-0.6Pct Cr Alloy, and Maraging Steel in Plastic Straining," *Met. Trans.* **6A** (1975) 839-851.

20. Y. Flom and R. J. Arsenault, "Interfacial Bond Strength in an Aluminum Alloy 6061-SiC Composite," *Mat. Sci. and Eng.* **77** (1986) 191-197.

21. M. E. Fine, "Dynamic Methods for Determining the Elastic Constants and Their Temperature Variation in Metals," **129** (1952) 43.

22. M. S. Zedalis, M. V. Ghate and M. E. Fine, "Elastic Moduli of Al_3Zr," *Scripta Met.* **19** (1985) 647-650.

23. M. M. Myshlyaev, W. A. Stepanov and V. V. Shpeizman, "Change in Creep Mechanism of B.C.C. Metals at Transition from Low to High Temperatures," *Phys. Stat. Sol.* **8** (1971) 393-402.

24. O. Izumi and D. Oelschlägel, "On the Decomposition of a Highly Supersaturated Al-Zr Solid Solution," *Scripta Met.* **3** (1969) 619-622.

25. E. Nes, "Precipitation of the Metastable Cubic Al_3Zr-phase in Subperitectic Al-Zr Alloys," *Acta Met.* **20** (1972) 499-506.

26. N. Ryum, "Precipitation and Recrystallization in an Al-0.5 Wt.% Zr-Alloy," *Acta Met.* **17** (1969) 269-278.

27. T. Haugan, E. Nes and N. Ryum, "Precipitation Reactions in Al-Z-Alloys," in: *Mat. Res. Soc. Symp.,* MRS, ed., Elsevier Science Publishing Co., Inc., 495-499.

28. J. E. Hatch, "Aluminum: Properties and Physical Metallurgy," in: ed., ASM, Metals Park (1984) .

29. V. C. Nardone and K. M. Prewo, "On the Strength of Discontinuous Silicon Carbide Reinforced Aluminum Composites," *Scripta Met.* **20** (1986) 43-48.

30. R. J. Arsenault, "The Strengthening of Aluminum Alloy 6061 by Fiber and Platelet Silicon Carbide," *Mat. Sci and Eng.* **64** (1984) 171-181.

31. V. C. Nardone and J. R. Strife, "Analysis of the Creep Rupture of Silicon Carbide Whisker Reinforced 2124 Al (T4)," *Met. Trans.* **18A** (1987) 109-114.

32. T. G. Nieh, "Creep Rupture of a Silicon Carbide Reinforced Aluminum Composite," *Met. Trans.* **15A** (1984) 139-146.

33. T. Morimoto, et al., "Second Stage Creep of SiC Whisker/6061 Aluminum Composite at 573K," *J. Eng. Mat. and Tech.* **110** (1988) 70-76.

34. S. Goto and M. McLean, "Modelling Interface Effects During Creep of Metal Matrix Composites," *Scripta Met.* **23** (1989) 2073-2078.

35. T. G. Nieh, K. Xia and T. G. Langdon, "Mechanical Properties of Discontinuous SiC Reinforced Aluminum Composites at Elevated Temperatures," *J. Eng. Mat. and Tech.* **110** (1988) 77-82.

36. Yen-Cheng Chen, "Thermal Stability of $L1_2$ structured $Al_3(Zr_xV_{1-x})$ in Rapidly Solidified Al-Zr-V Alloys," PhD Thesis, Northwestern University (1988).

37. B. J. Kestel, "Non-Acid Electrolyte Thins Many Materials for TEM Without Causing Hydride Formation," *Ultramicroscopy* **19** (1986) 205-212.

Figures

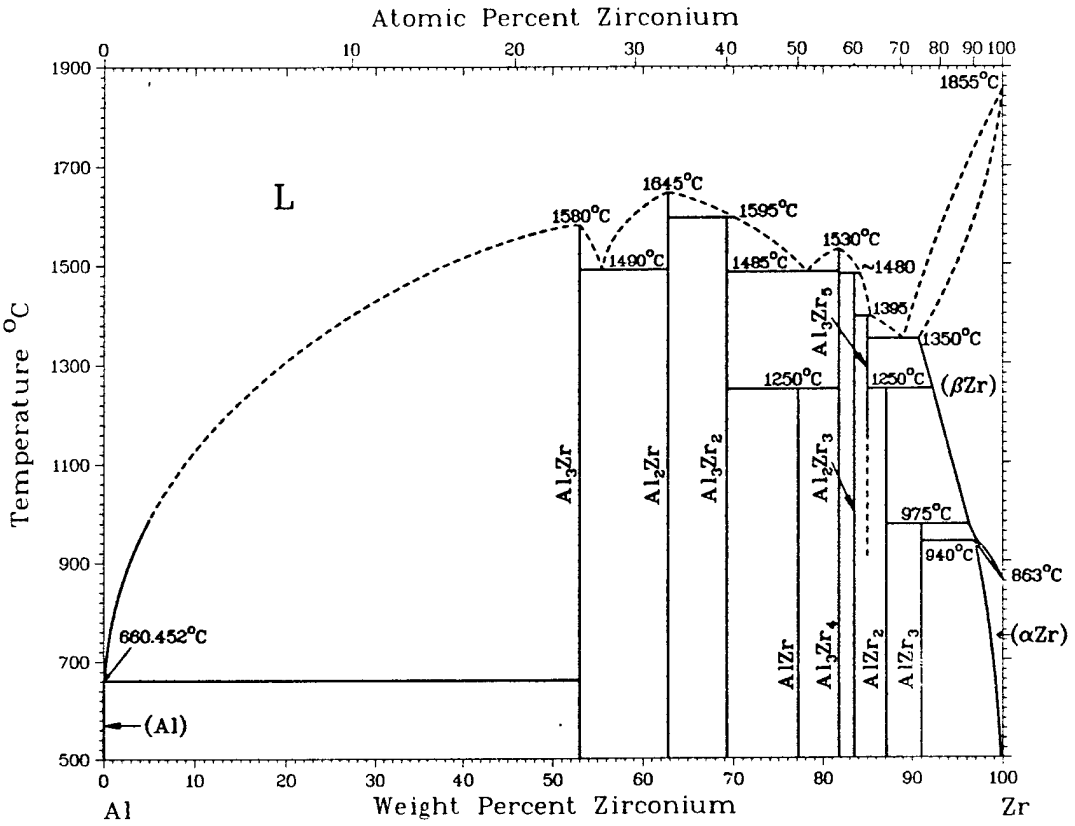

Fig. 1. Equilibrium Phase Diagram of the Al-Zr system.[12]

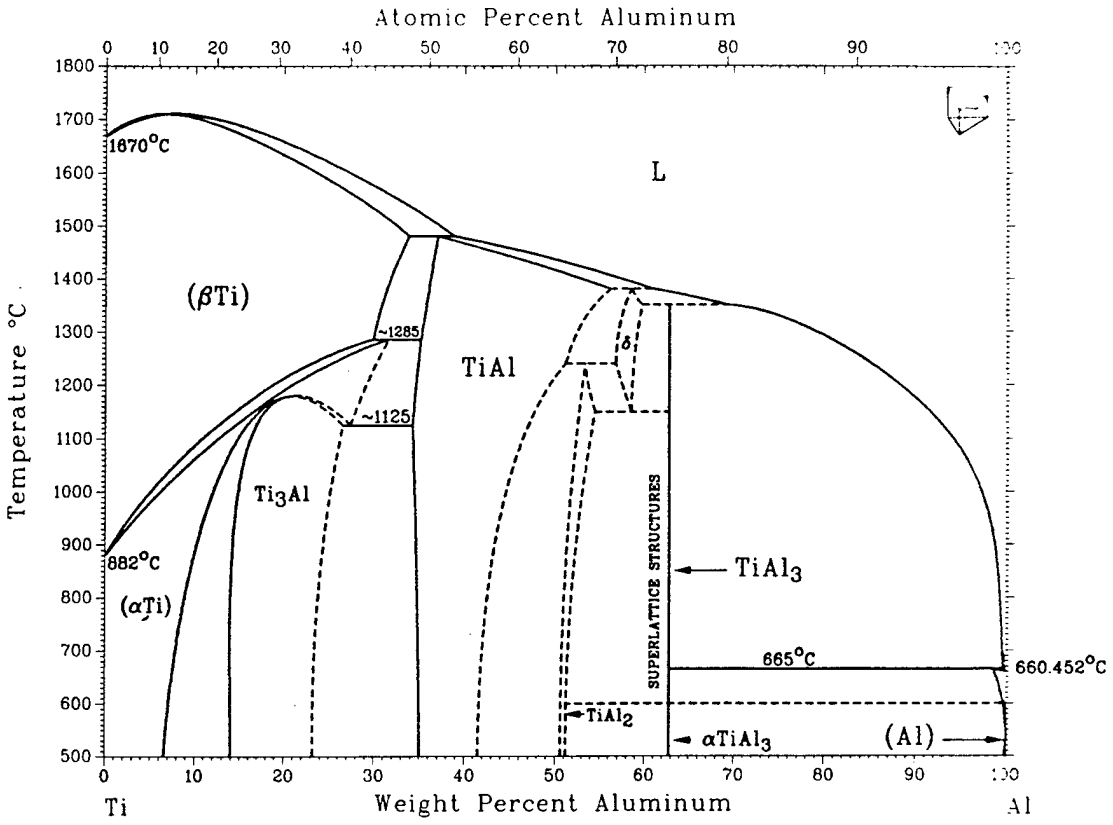

Fig. 2. Equilibrium Phase Diagram of Al-Ti system.[12]

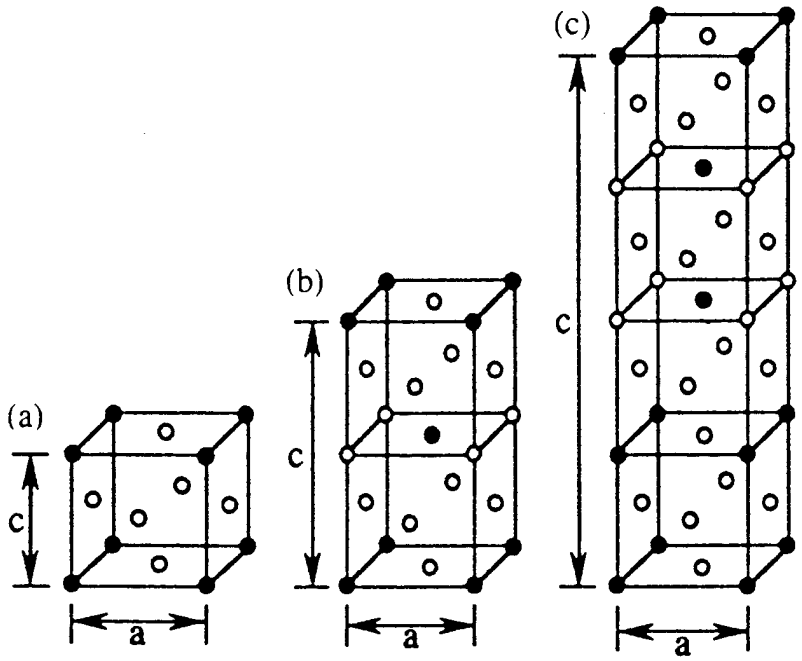

Fig. 3. a) FCC unit cell of Al. c=a; b) tetragonal DO_{22} structure; c)tetragonal DO_{23} structure[14]

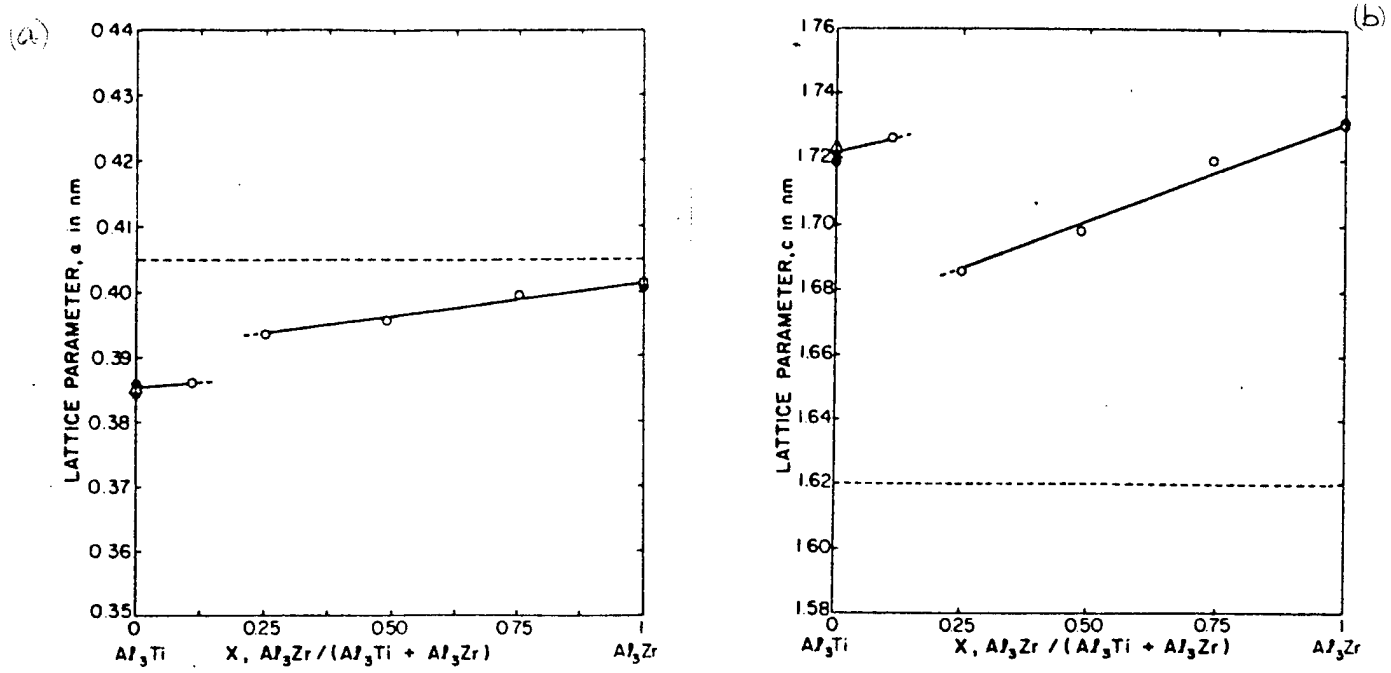

Fig. 4. Lattice parameters of a) a and b) c of $Al_3Zr_xTi_{1-x}$ [15].

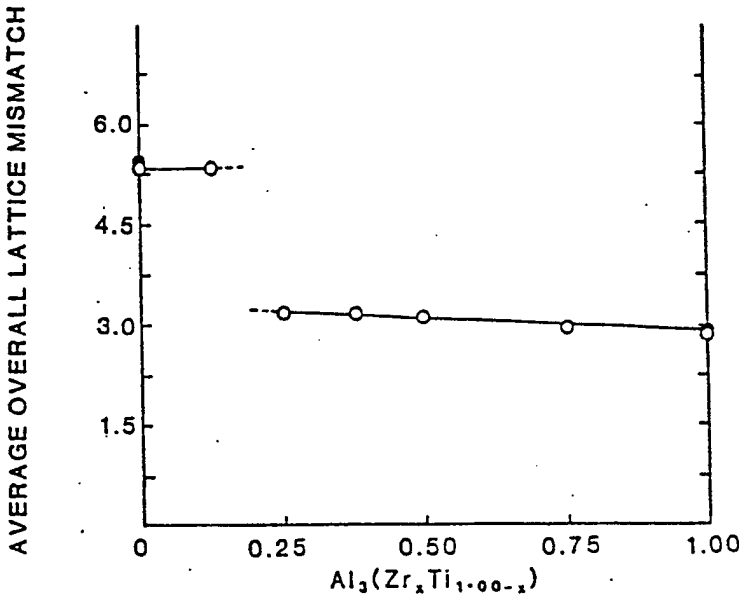

Fig. 5. Average Overall lattice mismatch in $Al_3Zr_xTi_{1-x}$ [11].

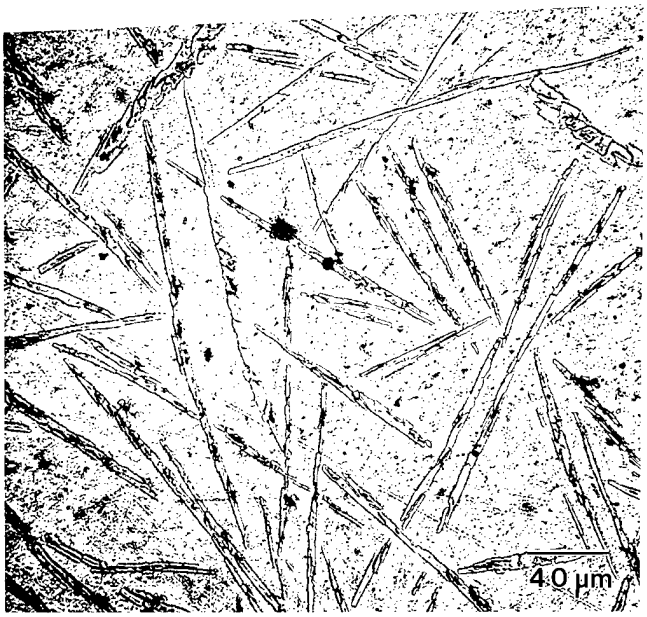

Fig. 6. Al/$Al_3Zr_{0.25}Ti_{0.75}$ (15 v/o). As-cast.

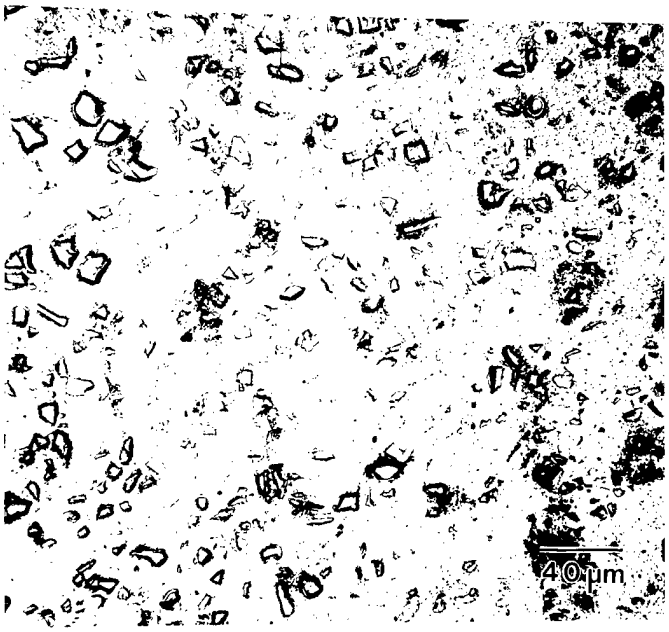

Fig. 7. Al/$Al_3Zr_{0.25}Ti_{0.75}$ (15 v/o). Hot-pressed and cold-rolled to 95% reduction. Longitudinal section.

Fig. 8. Al/$Al_3Zr_{0.25}Ti_{0.75}$ (15 v/o). Hot-pressed and cold-rolled to 95% reduction. Long transverse section.

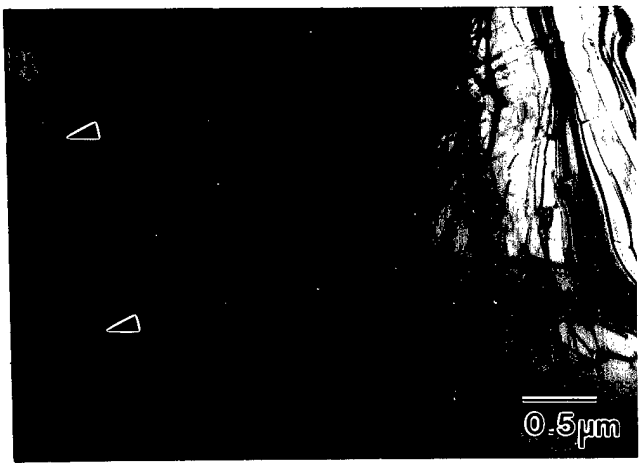

Fig. 9. Al/$Al_3Zr_{0.75}Ti_{0.25}$ (15 v/o). Electron micrograph of particle/matrix interface.

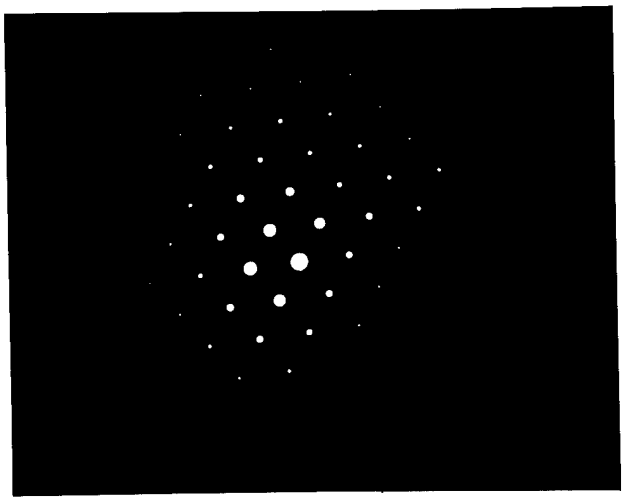

Fig. 10. Electron diffraction pattern of $Al_3Zr_{0.75}Ti_{0.25}$ particle above.

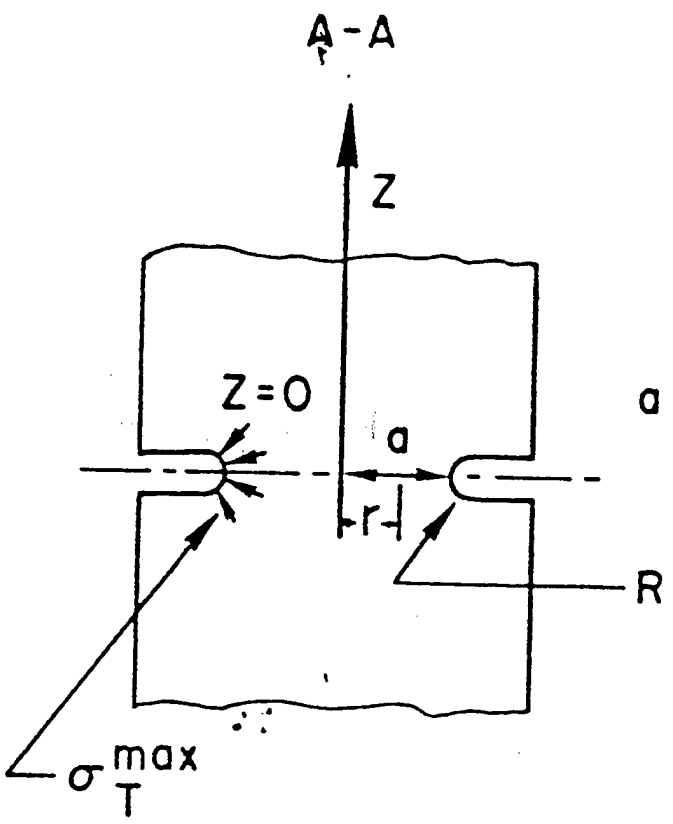

Fig. 11. Notched region in tensile specimen.[20]

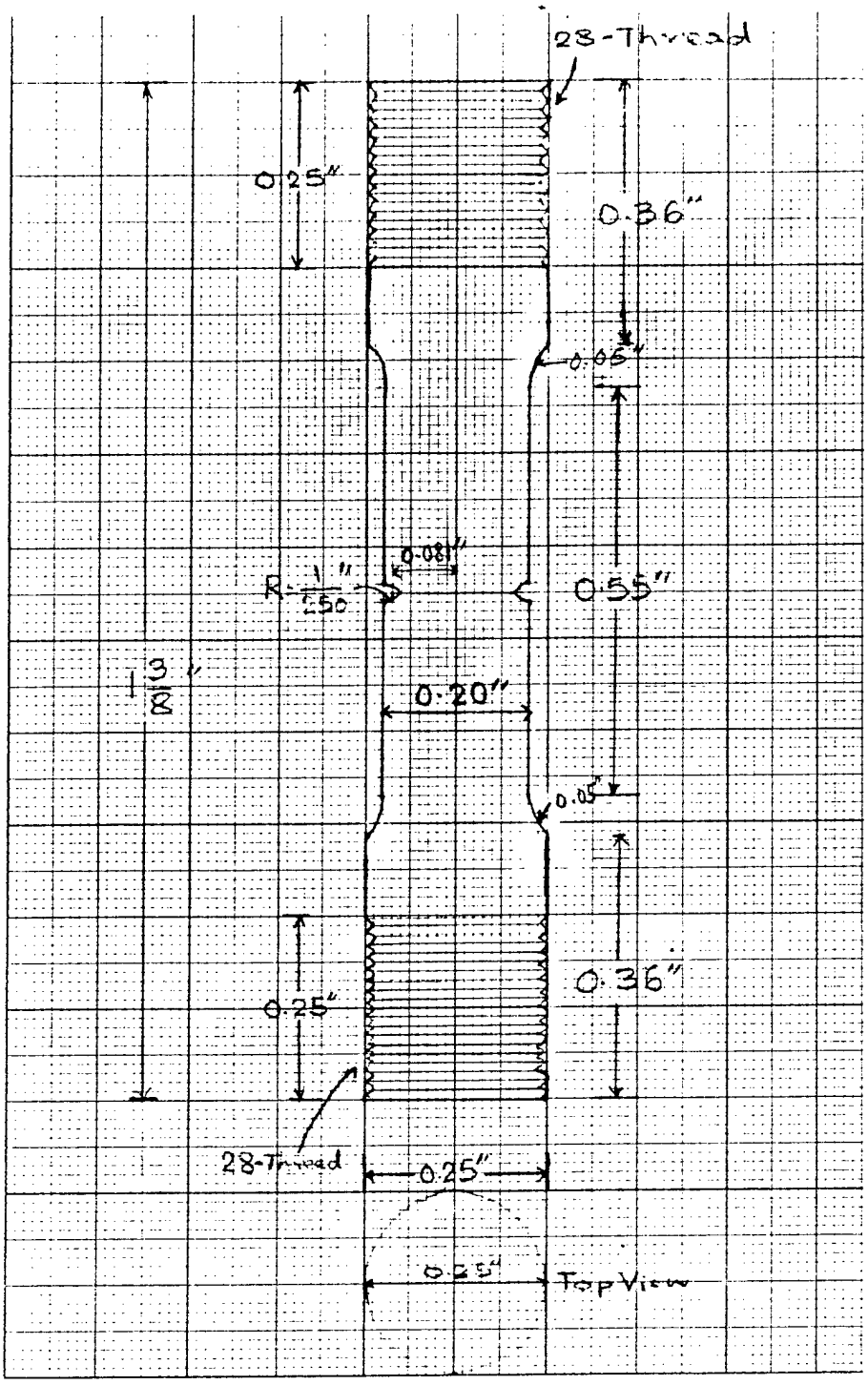

Fig. 12. Tensile specimens for interfacial strength test.

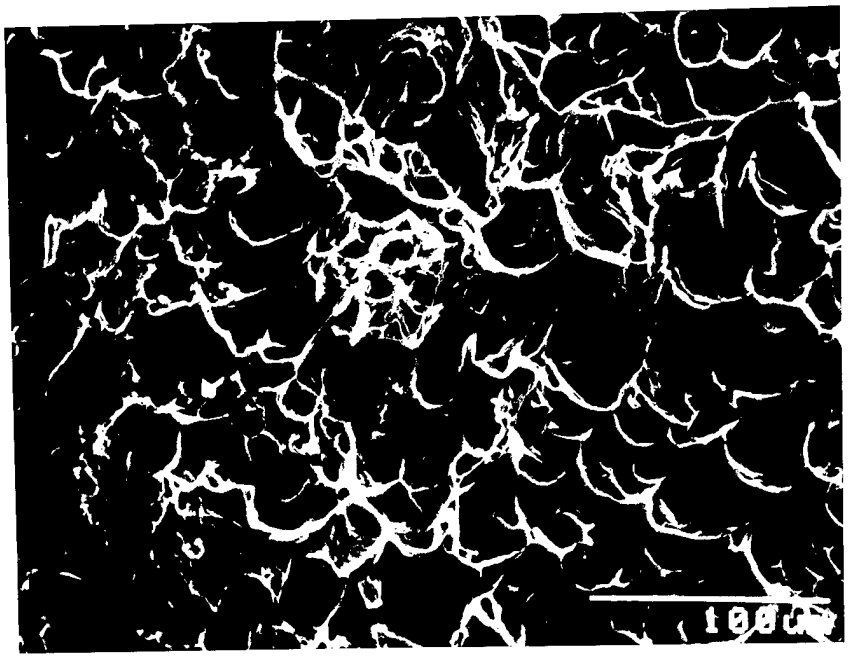

Fig. 13. Fracture surface of Al/$Al_3Zr_{0.25}Ti_{0.75}$ (3 v/o) sample tested in tension to failure.

Fig. 14. Young's Modulus vs. volume percent precipitate $Al_3Zr_{.5}Ti_{.5}$

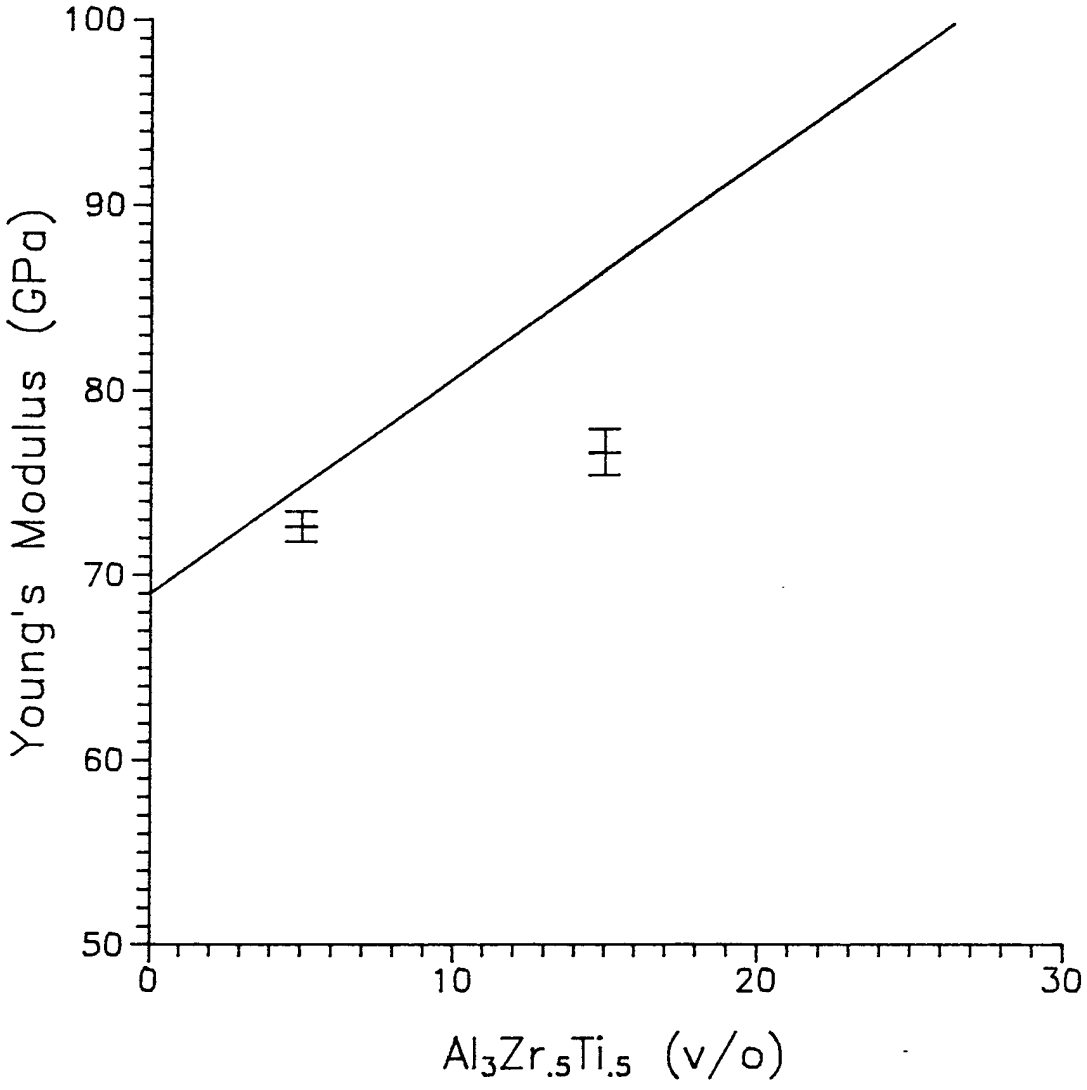

Fig. 15. Young's Modulus vs. volume percent precipitate $Al_3Zr_{.25}Ti_{.75}$

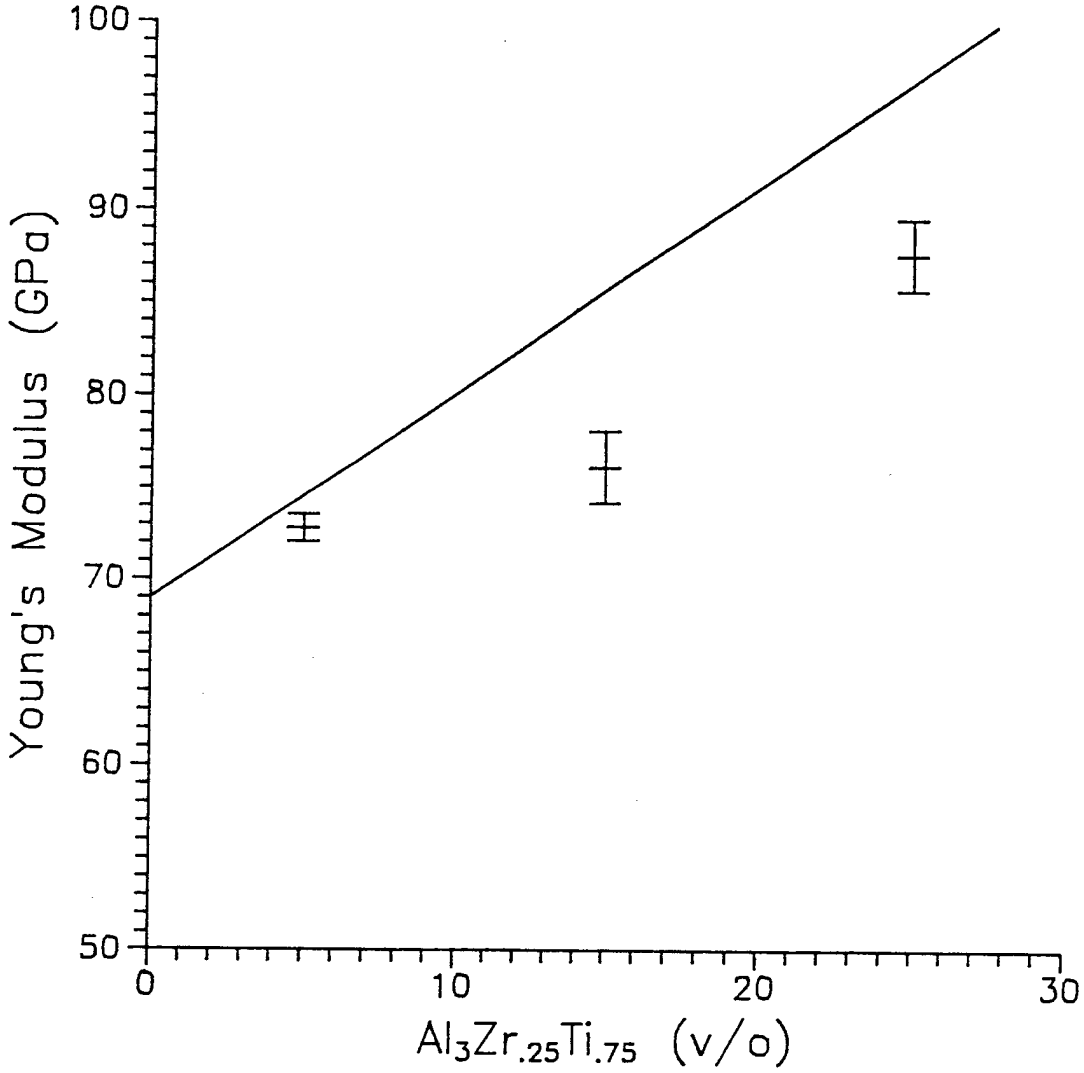

Fig. 16. Young's Modulus vs. Percent Porosity.
Al-Al3-Zr0.25-Ti0.75 (15 v/o). As-Cast.